Structural and Mechanical Properties of the ZrC/Ni-Nanodiamond Coating Synthesized by the PVD and Electroplating Processes for the Cutting Knifes

Article *in* Journal of Materials Engineering and Performance · April 2018

DOI: 10.1007/s11665-018-3362-2

Vadzim Chayeuski
Belarusian State Technological University

Valery Zhylinski
Belarusian State Technological University

Olegas Černašėjus
Vilnius Gediminas Technical University

Nikolaj Visniakov
Vilnius Gediminas Technical University

Structural and Mechanical Properties of the ZrC/Ni-Nanodiamond Coating Synthesized by the PVD and Electroplating Processes for the Cutting Knifes

V. Chayeuski, V. Zhylinski, O. Cernashejus, N. Visniakov & G. Mikalauskas

Journal of Materials Engineering and Performance

ISSN 1059-9495
Volume 28
Number 3

J. of Materi Eng and Perform (2019) 28:1278-1285
DOI 10.1007/s11665-018-3362-2

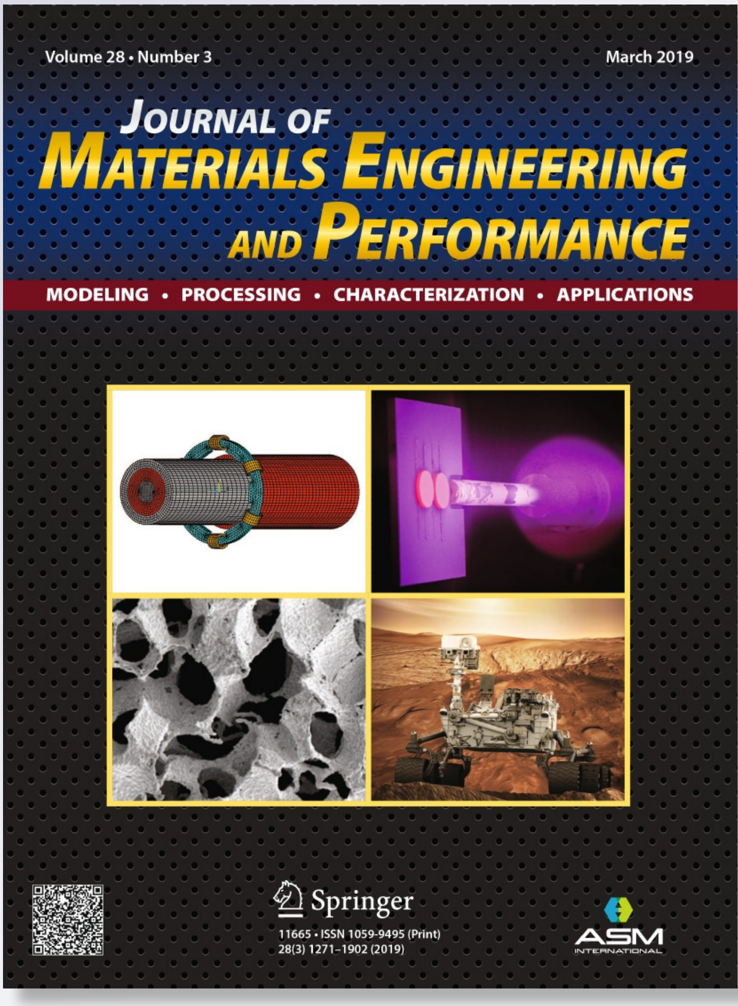

Springer

JMEPEG (2019) 28:1278–1285
https://doi.org/10.1007/s11665-018-3362-2

1059-9495/$19.00

Structural and Mechanical Properties of the ZrC/Ni-Nanodiamond Coating Synthesized by the PVD and Electroplating Processes for the Cutting Knifes

V. Chayeuski, V. Zhylinski, O. Cernashejus, N. Visniakov, and G. Mikalauskas

(Submitted November 20, 2017; in revised form March 22, 2018; published online April 17, 2018)

In this work, combined gradient ZrC/Ni-nanodiamond ultradispersed diamonds (UDD) coatings were synthesized on the surface of knife blades made of hard alloy WC-2 wt.% Co by electroplating and cathode arc evaporation PVD techniques to increase the durability period of a wood-cutting milling tool. The microstructure, phase and elemental composition, microhardness, and adhesion strength of the coatings were investigated. Ni-UDD layer is not mixed with the ZrC coating and hard alloy substrate. Cobalt is present in Ni-UDD layer after deposition of ZrC. The ZrC/Ni-nanodiamond coating consists of separate phases of zirconium carbide (ZrC), α-Ni, and Ni-UDD. The maximum value of microhardness of the Ni-nanodiamond coating is 5.9 GPa. The microhardness value of the ZrC/Ni-nanodiamond coatings is 25 ± 6 GPa, which corresponds to the microhardness of the hard alloy substrate and ZrC coating. The obtained high values of the critical loads on the scratch track of the ZrC/Ni-nanodiamond coating in 24 N prove a sufficiently high value of the adhesion strength of the bottom Ni-UDD layer with WC-Co substrate. Pilot testing of ZrC/Ni-nanodiamond-coated cutting tools proved their increasing durability period to be 1.5-1.6 times higher than that of bare tools, when milling laminated chipboard.

Keywords ceramics, coatings, inorganic, nanomaterials, structural

1. Introduction

Woodworking milling tool operates in conditions of static and dynamic loads, high temperatures, which causes increased wear of the cutting elements of the tool. To improve tool life, the cemented tungsten carbide is used (Ref 1, 2). Tail milling tool with the cutting edge profile plates made of tungsten carbide WC hard alloys is applied for cutting composite materials (laminates, laminated chipboard, etc.) (Ref 3). Unlike wood, the boards have a laminated structure with components that act as abrasives (Ref 4). Different types of chemical wear (corrosion and oxidation) of hard alloys based on WC-Co tools are proved to play a significant role in destruction of cutting edge blade during processing of plate wooden materials. This leads to pulling out of grain from the surface of tungsten carbide cutting element (Ref 5).

The coating protects the substrate against mechanical wear and corrosion while at the same time helping the cutting tool body to absorb mechanical stress, dissipating the heat, and promoting stress relief. It is known that an application of traditional hard ceramics, such as nitrides, carbides, and borides (TiC, ZrN, CrN, Mo-N, etc.), synthesized by the physical vapor deposition (PVD) or chemical vapor deposition (CVD) methods is used to strengthen a surface layers of the working areas of the cutting tools (Ref 6, 7). It is shown (Ref 8) that the tools with multilayer CrN/CrCN coatings improve wear resistance of the treated surface to be 2-3 times in comparison with uncoated knives when milling saw pinewood. Therefore, protective coatings having outstanding properties, such as the high hardness, low friction coefficient, low wear resistance, and chemical stability, are applied for carbide composite cutting tool. Nanostructured multilayered coatings such as CrZrN, Ti-(TiAl)N, TiCrN, (Ti-Zr-Nb)N synthesized by the PVD process, i.e., arc evaporation PVD, are found to possess superior mechanical and tribological properties (Ref 8-12). Thereby, the lifetime of carbide tools can be considerably improved.

On the other side, wood-cutting tools with the application of synthetic diamond were offered (Ref 13). Hard alloy cutting tool is tipped with polycrystalline diamond (PCD) segments that perform the cutting and prolong the life of the tool. PCD segments are increasingly used in woodworking due to extended tool life resulting from their superior properties over traditional tool materials. The use of nanodiamond (ultradispersed diamonds obtained by detonation of explosives) as a composite in electrochemical and chemical coatings also leads to an increase in their wear resistance, significant adhesion, and a significant decrease of the friction coefficient (Ref 14).

Ni and Cr electroplatings are used in engineering to improve wear resistance of tools (Ref 15). The positive side of the electrochemical processing of tool is simplicity of the technological operations of forming the electroplating layer, no high temperature in the manufacture of tools, and low-energy consumption installations. The main drawback of the modified tool electroplated alloy based on nickel is that the Ni matrix does not have high strength characteristics (Ref 16).

This article is an invited paper selected from presentations at "11th International Conference on Advanced Computational Engineering and Experimenting, ACE-X 2017," held July 3-6, 2017, in Vienna, Austria, and has been expanded from the original presentation.

V. Chayeuski and **V. Zhylinski**, Belarusian State Technological University, 13a, Sverdlov str., 220006 Minsk, Belarus; **O. Cernashejus, N. Visniakov,** and **G. Mikalauskas**, Vilnius Gediminas Technical University, 28, Basanaviciaus str., 03224 Vilnius, Lithuania. Contact e-mail: chaevskiv@gmail.com.

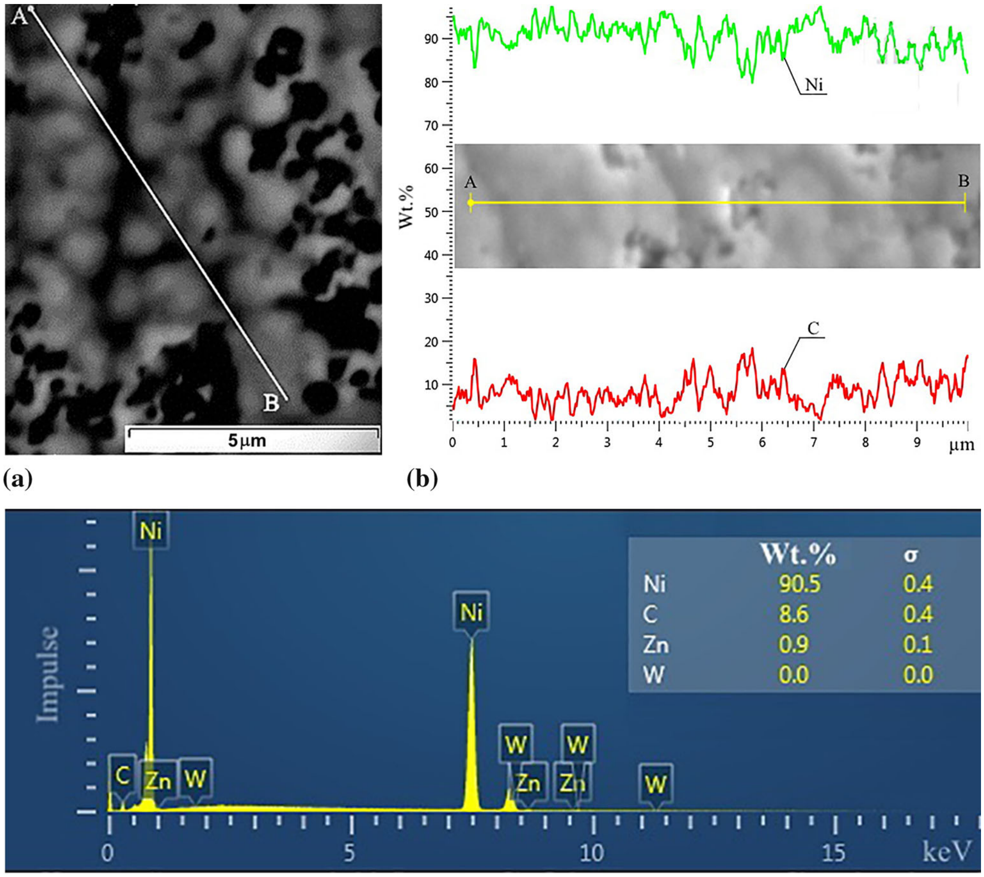

Fig. 1 Microstructure of the coated Ni-UDD surface: (a) SEM image of surface, (b) concentration distribution of elements (C, Ni) in surface layer during scanning along AB line over surface, and (c) EDS spectrum and elemental composition

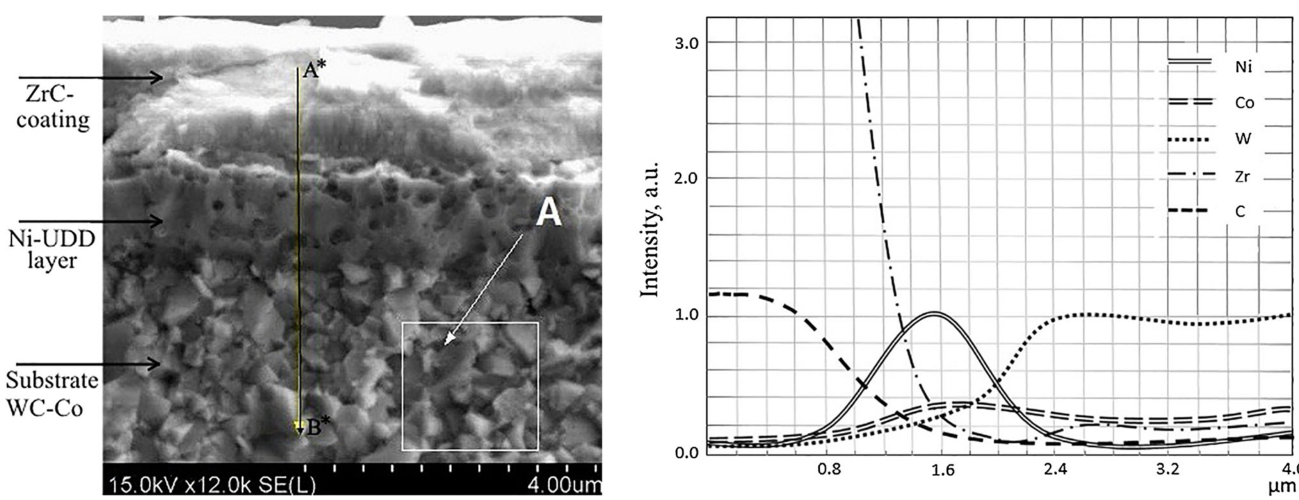

Fig. 2 Microstructure of the coated ZrC/Ni-nanodiamond hard alloy knife: (a) fracture cross-sectional views of the sample and the selected area A for EDS and (b) distribution of intensities of characteristic x-ray emission of elements (Ni, C, W, Zr, Co) in surface layer during scanning along line A^*B^* over surface

Cutting tools with double-layer ZrN/Ni-Co synthesized by the arc evaporation PVD and electroplating processes on hard alloy knives proved increase in their durability period for laminated chipboard milling (Ref 17).

Therefore, the aim of this work was to synthesize and investigate phase and elemental composition, microstructure, hardness, and adhesion strength of the ZrC/Ni-nanodiamond coatings on the surface of knife blades made of hard alloy WC-Co.

2. Experimental

2.1 Materials

The materials used were substrate and UDD. The substrate was a hard alloy knife made in Germany (Leitz company) (Ref 3). When preparing samples, UDD nanopowders of the detonation synthesis (nanodiamonds) with a particle size 4-6 nm were used (Ref 18). UDD particles have complex structure: a ~ 4 nm core of the classic cubic diamond and a carbon shell 0.4-1.0-nm thick around the core, which is made up of transition amorphous (according to x-ray diffraction data) carbon structures (Ref 19).

2.2 Methods

Ni-UDD composite electrochemical coatings were electroplated on the prepared surface of knives edges at direct current densities of 200-250 A/m^2 using sulfate-chloride electrolyte of nickel plating at the concentration of nanodiamonds in the electrolyte corresponding to 4.5 kg/m^3. The composition of electrolyte was the following (kg/m^3): $NiSO_4 \cdot 7H_2O$-30; $NiCl_2 \cdot 6H_2O$-4; H_3BO_3-3. The acidity (*pH*) of the electrolyte was measured by *pH*-meter 150-*pH* with accuracy of ± 0.05%.

Before the deposition of Ni-nanodiamond coating, the surface preparation of sample was carried out by chemical degreasing at the temperature 333-353 K for 360-480 s, rinsing in hot (313-333 K) and cold (291-228 K) water, etching in solution H_2SO_4 (5-10 kg/m^3) with inhibitor at the temperature 291-298 K, cold rinsing, activation, and washing.

Table 1 Chemical composition of tungsten carbide

Element	C	O	Co	W
Concentration, wt.%	11.5 ± 1.5	1.5 ± 0.3	2.0 ± 0.1	85.0 ± 3.0

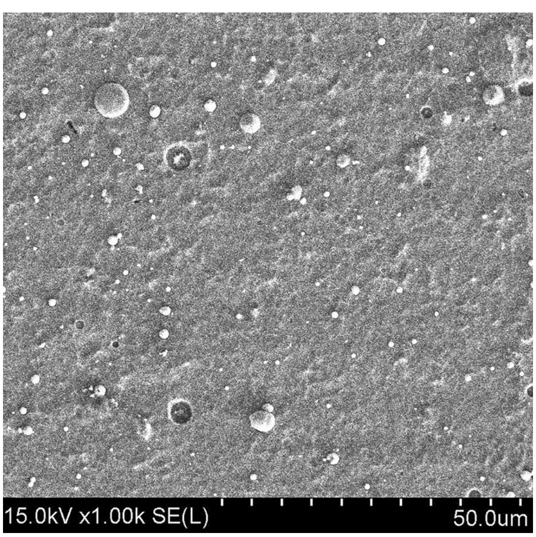

Fig. 3 Surface morphology of the ZrC/Ni-nanodiamond coating

The ZrC coating was deposited by the arc evaporation PVD method on the hard alloy WC-Co samples with Ni-nanodiamonds layer in two stages (Ref 7). At first, the surface of specimens was treated with zirconium ions for 60 s at a negative bias of 1 kV, the cathode arc burning current of 100 A, and the vacuum in the chamber 10^{-3} Pa. This stage resulted in heating the substrate to 723-773 K prior to deposition. Then, coating was precipitated for 600 s at CH_4 pressure of 10^{-1} Pa in the chamber under a bias of − 120 V.

The microstructure of the coating, the edges of the knives, and the surface morphologies of the coatings were analyzed for the wafer surface samples and samples fracture, using methods of energy-dispersive x-ray spectroscopy (EDS) and scanning electron microscopy (SEM) by Hitachi S-4800 and LEO-1455VP electron microscopes (Japan).

The phase composition of coatings was investigated with x-ray diffraction (XRD) using Cu-K_α characteristic of x-ray radiation. The XRD measurements were performed using the Ultima IV diffraction meter (Japan).

The microhardness of surface layers was measured by the Vickers technique using a diamond pyramid under load of 0.5-1.0 N. The microhardness instrument was AFFRI-DM8 (Italy) with an accuracy of ± 15 HV.

The scratch resistance of the coated sample was tested with the Scratch Tester, which has a conical-shaped diamond indenter tip with a radius of curvature of 0.5 × 10^{-3} m. The speed of the indenter was 3.3 × 10^{-4} m/s. The maximum load on the indenter at the end of the track was up to 150 N.

The pilot tests of coated knives blades when milling laminated chipboard were carried out with the processing center ROVER B4.35 (Italy), using a mill with a diameter of 21 × 10^{-3} m with mechanical fastening of the cutting element. Laminated chipboard with a thickness of 25 × 10^{-3} m was milled. The computer numerical control (CNC) processing center is used at the following modes: the frequency of rotation of milling cutters—200 s^{-1}; feed rate—0.07 m/s; machining allowance—5.0 × 10^{-3} m/pass; average chip thickness—0.15 × 10^{-3} m. Appearance of defects on the treated surface was the criteria of losing the cutting ability of the cutting element. The main type of defect was laminate chipped from the plate surface.

3. Results and Discussion

3.1 Microstructural Analysis and Surface Morphology

In Fig. 1(a), the microstructure of the Ni-UDD composite electrochemical coating shows morphology in the form of globular formations, formed by clusters of nanodiamonds (Ref 16). The nanodiamond clusters are centers of deposition of nickel ions. The SEM images of the Ni-nanodiamond coating are shown in Fig. 1(b) and (c). Figure 1(b) reveals that carbon is present in the Ni-UDD layer in the form of linked agglomerates with the size of 0.7-2.5 μm. The previous studies reported the formation of clusters of nanodiamonds to be with the size up to 10 μm (Ref 16). The EDS spectrum of the Ni-

Table 2 Elemental composition of the ZrC-coating surface

Element	C	O	Ni	Zr
Concentration, wt.%	14.9 ± 2.5	3.6 ± 0.8	1.1 ± 0.1	80.4 ± 3.6

(a)

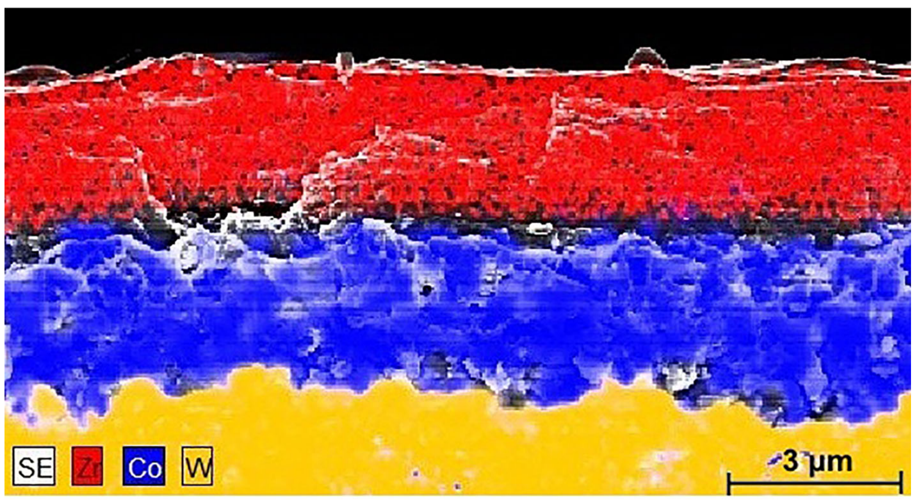

(b)

Fig. 4 SEM image of fracture cross section of the coated ZrC/Ni-nanodiamond knife and EDS maps of (a) Zr, Ni, W, and (b) Zr, Co, W

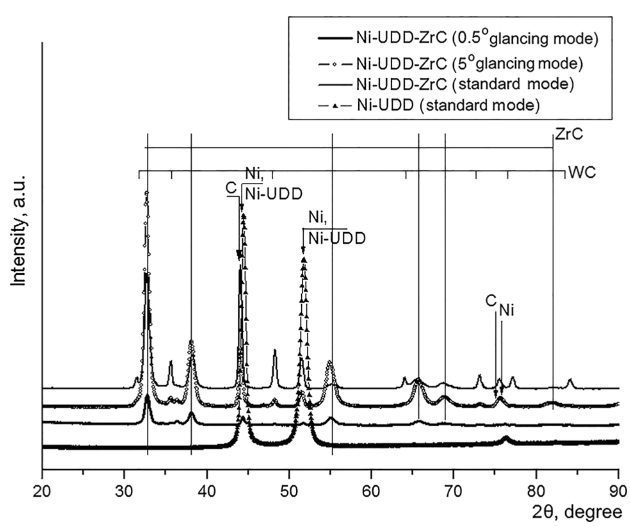

Fig. 5 XRD patterns for the ZrC/Ni-nanodiamond coating

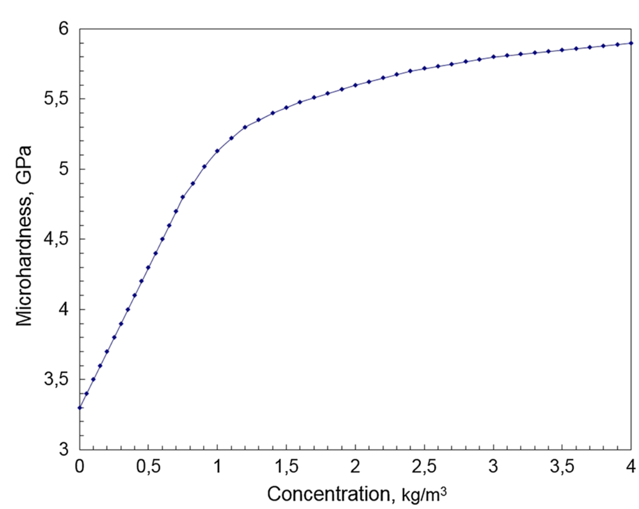

Fig. 6 Dependence of microhardness of Ni-nanodiamond coating on nanodiamond content in electrolyte

nanodiamond coating (Fig. 1c) shows that the Ni-UDD layer does not mix with the hard alloy substrate WC-Co.

Figure 2 shows the SEM image and microstructure of the fracture of cross section of the coated ZrC/Ni-nanodiamond hard alloy substrate WC-Co. The Nickel-nanodiamond layer is characterized by the structure with the presence of pores and voids, and it is not mixed with a hard alloy substrate and ZrC coating. Figure 2(a) shows individual coating thickness obtained for ZrC (top layer) and Ni-UDD (bottom layer) is 1.75 and 1.50 µm, respectively. Based on the EDS in a selected area of A substrate, as shown in Fig. 2(a), the chemical composition of the hard alloy substrate is presented in Table 1. In the result, we can conclude that carbide base has a crystalline structure and consists of tungsten carbide WC-2 wt.% Co. The resulting conclusion confirms the results of studies (Ref 17, 20).

The surface morphology of the ZrC/Ni-nanodiamond coating is shown in Fig. 3. Here, it can be seen that the surface is rough. The coated surface shows a pattern with pits, pores, and dots (particles). These aspects are characteristics of the arc evaporation PVD deposition (Ref 21). Due to the high current densities during the arc evaporation process, a certain amount of the target material is ejected as small liquid droplets. The formation of macro-particles from droplets results in rough surface (Ref 22).

Analysis of the elemental composition of the surface of the ZrC/Ni-nanodiamond coatings presented in Table 2 helps us to conclude that the ZrC coating covers the Ni-UDD layer completely. Figure 4 shows EDS maps of the distribution of the elements within a fracture cross section of the samples after deposition of the zirconium carbide (ZrC), Ni-UDD layer. Figure 4(a) shows the presence of the Ni-UDD layer. SEM image (Fig. 4b) shows the presence of cobalt in the Ni-UDD layer, which is formed during deposition of the ZrC coating. The release of pure cobalt phase from the grains of hard alloy WC-Co is caused by the possibility of thermal diffusion of cobalt onto surface of hard alloy WC-Co (Ref 23). The pure nickel phase of Ni-nanodiamond coating interacts with the metal cobalt with the formation of continuous solid solutions with high strength characteristics (Ref 23, 24).

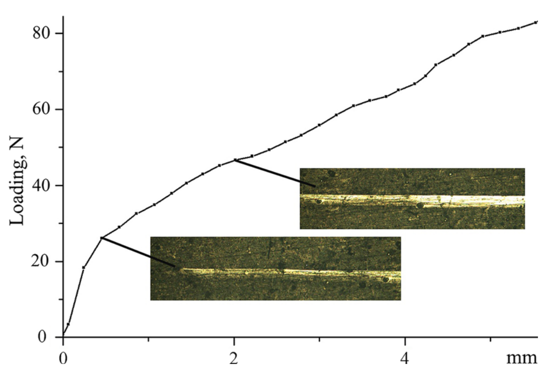

Fig. 7 Micro-scratch curve and scratch track pictures of the sample

3.2 Phase Analysis

The XRD patterns of the ZrC/Ni-nanodiamond coating are shown in Fig. 5. The coating exhibits a polycrystalline pattern for ZrC, Ni, Ni-UDD with mixed orientation. The high peaks in the 2θ ranging from 44° to 52° correspond to the Ni and Ni-UDD patterns. The observed peaks of nickel belong to the phase of cubic nickel with the FCC lattice. The Ni (111) peak at 44.5° is more intense than the Ni (200) peak at 51.8°. This aspect is characteristic of coatings containing Ni-UDD (Ref 25). Moreover, the diamond (111) high peak exists at 43.9°.

The 5° glancing XRD pattern of the deposited ZrC reveals the fine crystallinity of ZrC. There are wide low (200), (220), (311), and (222) peaks at 37.8°, 54.5°, 64.9°, and 68.2°, respectively. The ZrC (111) plane at 32.6° has shown a high peak (dominant orientation).

Therefore, the ZrC/Ni-nanodiamond coating consists of separate following phases: ZrC phase, nickel phase, and Ni-UDD phase.

3.3 Microindentation

The penetration of the diamond indenter tip was restricted to less than 1.0 µm of the coating thickness, in order to preclude any effects of the substrate response. When the concentration of ultradispersed diamonds increases from 1.0 to 4.0 g/m^3 in the electrolyte (Fig. 6), the microhardness of coating is increased from 5.1 to 5.9 GPa, associated with the increase in the degree of implementation of ultradispersed diamonds in the Ni-matrix. The obtained maximum values of microhardness of the Ni-nanodiamond coating (5.9 GPa) at a concentration of UDD in the electrolyte 4 kg/m^3 correspond to the data (Ref 16, 25). However, at such concentration of nanodiamonds, their quantitative content in the coating is much less than 1 wt.%, because obtained data prove the concentration of UDD 13 kg/m^3 of their quantitative content in the coating to be ~ 1 wt.% (Ref 25).

Therefore, the limit values of microhardness of the Ni-nanodiamond coating are not achieved and can be increased by increasing the concentration of nanodiamonds in nickel matrix or by a more uniform distribution of nanodiamonds in the nickel.

Studies have proved that coatings made of nano-size crystallites of NbC and Cu with a sublayer of NbC0.7 on hard alloy wood-cutting tool had high microhardness 44-35 GPa [26]. The hardness of the synthesized Cr-N interlayers of

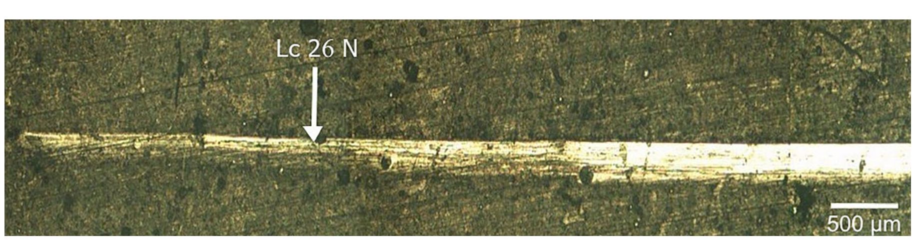

Fig. 8 Optical microscopy image from the scratch track of the ZrC/Ni-nanodiamond coating

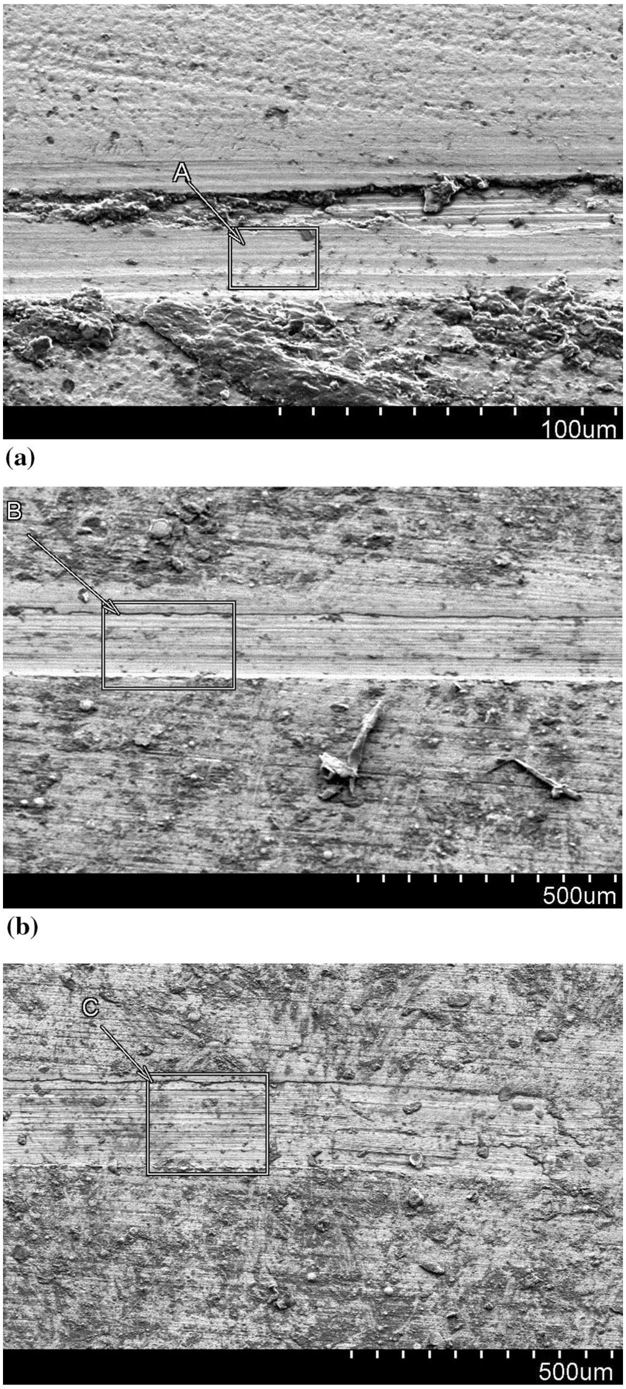

Fig. 9 SEM micrographs of the scratch track of the ZrC/Ni-nanodiamond coating: (a) cohesive path failure, (b) adhesive path failure in the middle, and (c) adhesive path failure in the end of scratch track

CrZrN coatings on a WC-6 wt.% Co substrate was measured to be in the range of 7-28 GPa (Ref 9). The microhardness value of ZrC/Ni-nanodiamond coatings is 25 $\pm$ 6 GPa, which corresponds to the microhardness (21 $\pm$ 2 GPa) of the hard alloy substrate (knife mills of Leitz company) and the ZrC coating (25-32 GPa) (Ref 17, 27), and also multicomponent coatings containing interlayers based on carbides, chromium, etc. (Ref 9, 26).

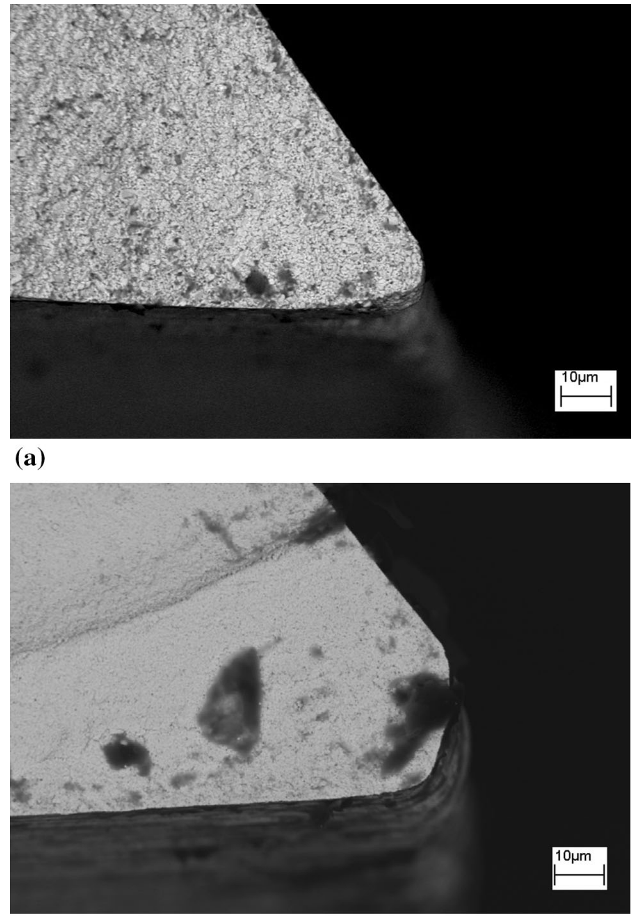

Fig. 10 SEM images of fractures of hard alloy knife (a) before and (b) after pilot tests when cutting laminated chipboards

3.4 Scratch Test Analysis and Pilot Tests

According to the obtained experimental data of the tribological tests of the ZrC/Ni-nanodiamond coatings on the Scratch Tester, the coating is destructed when the load reaches 26 $\pm$ 1 N, which corresponds to the bend and further same slope of the curve of microscratch, as shown in Fig. 7. As a result (Fig. 8), the indenter with further increase in the load begins to slide on the surface of the carbide WC-Co base. The obtained values of the critical loads on the scratch track of the coating in 26 N prove a sufficiently high value of the adhesion strength of the bottom Ni-UDD layer with hard alloy WC-Co substrate (Ref 9), suggesting the adhesion strength of the ZrC/Ni-nanodiamond coating to be sufficient for industrial application (Ref 9, 28).

Scratch track studies by analyzing SEM images of the scratch channel are presented in Fig. 9(a), (b), and (c). In the beginning of scratch track, the width and shape of the cohesive failure path into ZrC/Ni-nanodiamond coating show nonuniformities that can be assigned to the surface roughness (Fig. 9a). Besides, there are some delaminated coating areas (A) inside the scratch channel of ZrC/Ni-nanodiamond coating. The formation of the cracks inside of the scratch channel and on the edges of channel indicates brittle damages of coating under progressive loading of the diamond stylus. The scratch morphology of the coating, shown in the middle of track in

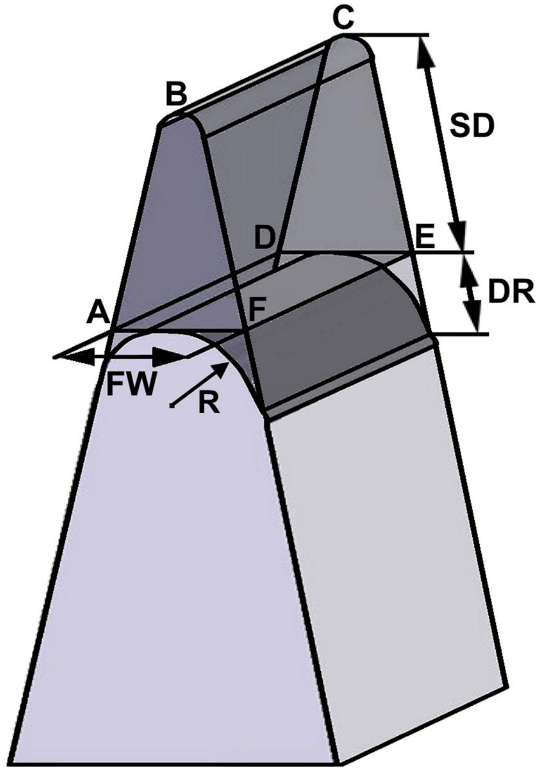

Fig. 11 Scheme for calculating the total wear of the cutting edge knife: worn edge displacement (SD), rake face wear (DR), and worn front-end width (FW)

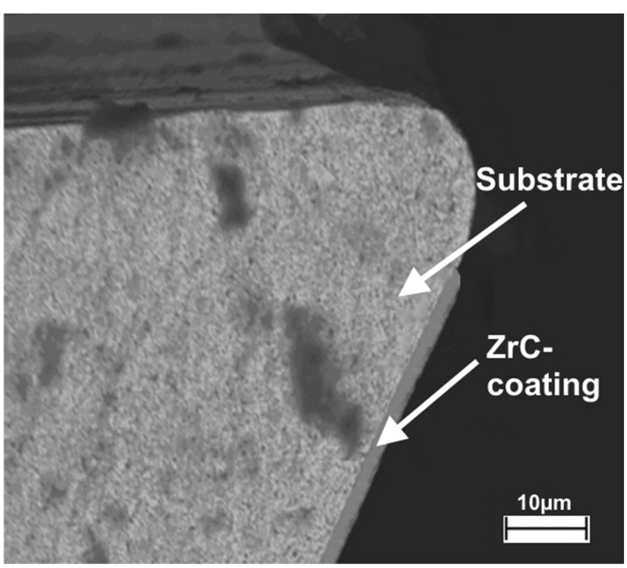

Fig. 12 SEM image of fracture of edge knife coated ZrC/Ni-UDD after pilot tests when cutting laminated chipboards

Table 3 Volume wear of hard alloy knives modified by coatings after tests of cutting laminated boards

Machining type	Volume wear, 10^6, μm^3
Bare edge knife	2.4 ± 0.2
ZrC/Ni-UDD coating	1.5 ± 0,1

Fig. 9(b), and corresponding to it, area B is smooth and even. The absence of a crack formation reveals the ductile damage behavior of these coatings in which the stresses were uniformly distributed in the vicinity of the diamond stylus during the scratch test. Furthermore, the trace of the head of the stylus on substrate is quite evident and shows that the coating is practically completely expelled (Fig. 9b). Furthermore, as visible in Fig. 9(b), the width of the scratch channel is considerably wider than the width of the adhesive failure path into coating (Fig. 9a), achieving the maximum meaning in the end of the scratch (Fig. 9c). The edges of the scratch path are quite smooth indicating a brittle fracture of the coating under the stylus pressure. Figure 9(c) shows that in the end of scratch track, absolute adhesive failure of the coating that is caused by chipping damages is not observed (area C).

Due to their unique structure (alternating layers of different composition, the presence of the solid carbide zirconium ZrC) and its high adhesion strength, the ZrC/Ni-nanodiamond coatings can be used to increase the durability period of a wood-cutting milling tool when cutting chipboard by CNC machines.

Figure 10 shows the SEM images of the cross-sectional fracture of the edge knife before (Fig. 10a) and after (Fig. 10b) pilot tests when cutting laminated chipboards. There is a significant dulling of the cutting edge after the tests. Figure 11 shows a diagram explaining the total wear of the knife cutting edge. From the explanatory scheme of worn edge knives (Fig. 11), we can see that the total wear of the cutting edge is a worn edge displacement (SD), rake face wear (DR), and worn front-end width (FW). This total wear of knife cutting edge was defined by means of the program of processing of SEM images of 3-5 pieces of knives (Fig. 10). The image of the fracture of the blade of a knife with a Zr/Ni-UDD coating (Fig. 12) proves that the degree of dulling after coating deposition is significantly less than in the case of a blade without coating (Fig. 10b). The performed estimates of the volumetric wear of the knives blade after pilot tests of modified cutters (Table 3) show that the volumetric wear of the blade with ZrC/Ni-UDD coating is reduced in 1.5-1.6 times compared with the blade without coating. The performed estimates of the volumetric wear of the knives blade after pilot tests of modified cutters are consistent with the obtained values of the total actual path of the contact of the knife with the processed material for the cutter with and without coating.

Thus, pilot tests of ZrC/Ni-nanodiamond-coated cutting tools proved their increasing durability period to be 1.5-1.6 times higher than that of bare tools, when milling laminated chipboard.

4. Conclusion

Combined gradient ZrC/Ni-nanodiamond coatings are formed on hard alloy tungsten carbide WC-2 wt.% Co for knives of cutting tools by the arc evaporation PVD and electroplating methods.

Nanodiamonds are distributed on the surface of the Ni-UDD layer in the form of clusters as the result of the adhesion activity of nanodiamond particles and their ability to form clusters to be 10 μm in size.

Ni-UDD layer is characterized by the structure with the presence of pores, and it is not mixed with the ZrC coating and hard alloy substrate. Cobalt is present after deposition of ZrC in Ni-UDD layer.

The ZrC/Ni-nanodiamond coating consists of the following separate phases: ZrC phase, nickel phase, and Ni-UDD phase.

The maximum value of microhardness of the Ni-nanodiamond coating (5.9 GPa) obtained at a concentration of UDD in the electrolyte is 4 kg/m^3. The microhardness value of the ZrC/Ni-nanodiamond coatings is 25 $\pm$ 6 GPa, which corresponds to the microhardness of the hard alloy substrate (knife mills of Leitz company) and ZrC coating.

The obtained high values of the critical loads on the scratch track of the ZrC/Ni-nanodiamond coating in 26 N prove a sufficiently high value of the adhesion strength of the intermediate Ni-UDD layer with hard alloy WC-Co substrate.

Held pilot tests of ZrC/Ni-nanodiamond-coated cutting tools proved their increasing durability period to be 1.5-1.6 times higher than that of bare tools, when milling laminated chipboard. The obtained results can be explained by unique structure of the ZrC/Ni-nanodiamond coating and its high adhesion strength.

Acknowledgments

The authors wish to acknowledge the financial support from the Ministry of Education of the Republic of Belarus through the Fund for Fundamental Research of the Republic of Belarus (project No 7.4 "Galvanotechnics," assignment No 7.4.6).Besides that, the authors are grateful to science group of the State Center "Belmikroanaliz" (the branch Scientific and Technical Center "Belmikrosistemy" of "INTEGRAL" Holding, the Republic of Belarus) for performing part of this work and for helpful discussion.

References

1. F.E. Palomar, P.C. Zambrano, M.I. Gómez, R. Colás, M.P. Guerrero, and A. Castillo, Coatings Made of Tungsten Carbide and Tantalum Carbide for Machining Tools, *Vacuum*, 2010, **84**, p 1236–1239
2. K. Egashira, S. Hosono, S. Takemoto, and Y. Masao, Fabrication and Cutting Performance of Cemented Tungsten Carbide Micro-Cutting Tools, *Precis Eng*, 2011, **35**(4), p 547–553
3. LEKSIKON Leitts: catalog firmy Leitz (LEKSIKON Leitz: Leitz Co. Catalog), on CD-ROM, Moscow, *Leitts Instrumenty*, 2011, (**in Russian**)
4. V.V. Abrazumov and V.D. Kotenko, The Analysis of the Phenomena on Contact Surfaces of a Cutting at cutting Board Wood Composite Materials, *Vestnik Moskovskogo gosudarstvennogo universiteta lesa, For Bul*, 2006, **6**, p 138–141 (**in Russian**)
5. V.V. Abrazumov, Wear resistance of cutting tools during machining of wooden composite materials, Doctoral (Eng.) Thesis, Moscow State Forest University, 2009 (**in Russian**)
6. G. Ma, L. Wang, G. Haoxiang, J. Zhang, and T. Reddyhoff, The Friction Coefficient Evolution of a TiN Coated Contact During Sliding Wear, *Appl. Surf. Sci.*, 2015, **345**, p 109–115
7. A.K. Kuleshov, V.V. Uglov, D.P. Rusalsky, A.A. Grishkevich, V.V. Chaevski, and V.N. Haranin, Effect of ZrN and Mo-N Coatings and Sulfacyanization on Wear of Wood-Cutting Knives, *J. Frict. Wear*, 2014, **35**(3), p 201–209
8. A. Gilewicz, B. Warcholinski, P. Myslinski, and W. Szymanski, Anti-wear Multilayer Coatings Based on Chromium Nitride for Wood Machining Tools, *Wear*, 2010, **270**, p 32–38
9. H.K. Kim, J.H. La, K.S. Kim, and S.Y. Lee, The Effects of the H/E Ratio of Various Cr-N Interlayers on the Adhesion Strength of CrZrN Coatings on Tungsten Carbide Substrates, *Surf. Coat. Technol.*, 2015, **284**, p 230–234
10. V.M. Beresnev, S.S. Grankin, S.Y. Novikov, U.S. Nyemchenko, O.V. Sobol, and P.V. Turbin, Tribotechnical Properties of the Coatings (Ti-Zr-Nb)N, *J. Nano-Electron. Phys.*, 2014, **6**(4), p 4011–4015
11. T.S. Kumar, S.B. Prabu, and G. Manivasagam, Metallurgical Characteristics of TiAlN/AlCrN Coating Synthesized by the PVD Process on a Cutting Insert, *J. Mat. Eng. Perf.*, 2014, **23**(8), p 2877–2884
12. S.N. Grigoriev, A.A. Vereschaka, S.V. Fyodorov, N.N. Sitnikov, and A.D. Batako, Comparative Analysis of Cutting Properties and Nature of Wear of Carbide Cutting Tools with Multi-Layered Nano-Structured and Gradient Coatings Produced by Using of Various Deposition Methods, *Int. J. Adv. Manuf. Technol.*, 2017, **90**(9–12), p 3421–3435
13. P. Philbin and S. Gordon, Characterisation of the Wear Behaviour of Polycrystalline Diamond (PCD) Tools when Machining Wood-Based Composites, *J. Mater. Proces. Technol.*, 2005, **162–163**, p 665–672
14. V.Y. Dolmatov, Detonation Synthesis Ultradispersed Diamonds: Properties and Applications, *Rus. Chem. Rev.*, 2001, **70**(7), p 687–708
15. S.S. Popova, G.V. Tseluikina, N.D. Solovieva, and V.N. Tseluikin, Functional Coatings Based on Iron Alloys, *Electroplat. Surf. Treat.*, 2001, **9**(1), p 34–39 (**in Russian**)
16. N.I. Polushin, A.V. Kudinov, V.V. Zhuravlev, N.N. Stepareva, and A.L. Maslov, Dispersed Hardening of Diamond Composite Electrochemical Coating by Nanoparticles, *Rus. J. Non-Ferr. Met.*, 2013, **54**(5), p 412–416
17. V. Chayeuski, V. Zhylinskiy, A. Grishkevich, P. Rudak, and S. Barcik, Influence of High Energy Treatment on Wear of Edges Knives of Wood-Cutting Tool, *MM Sci. J.*, 2016, **6**, p 1519–1523
18. A.S. Kononov, Y.S. Sachivko, A.P. Korzhenevskiy, and R.G. Shtemplyuk, Thermal Stability of Chromium Coatings Modified with Nano-Sized Oxygen-Containing Additives, *Mechanics of Machines, Mechanisms and Materials*, 2015, **4**, p 353–357
19. G.K. Burkat and V.Y. Dolmatov, Application of Ultrafine-Dispersed Diamonds in Electroplating, *Phys. Solid State*, 2004, **46**(4), p 703–710
20. A.V. Alifanov, A.A. Grishkevich, V.V. Chayevskii, and V.N. Garanin, Influence of TiN-Coatings Hard Alloy Knives on Exploitation of Wood-Cutting Milling Tool when Processing Laminated Chipboard, *Proc. BSTU*, 2012, **2**, p 146–149
21. A.A. Matei, I. Pencea, S.G. Stanciu, R. Hristu, I. Antoniac, E. Ciovica, C.E. Sfat, and G.A. Stanciu, Structural Characterization and Adhesion Appraisal of TiN and TiCN Coatings Deposited by CAE-PVD Technique on a New Carbide Composite Cutting Tool, *J. Adhesion Sci. Tech.*, 2015, **29**(23), p 2576–2589
22. S.W. Huang, M.W. Ng, M. Samandi, and M. Brandt, Tribological Behaviour and Microstructure of $TiC_xN_{(1-x)}$ Coatings Deposited by Filtered Arc, *Wear*, 2002, **252**, p 566–579
23. K. Chen, L. Zhao, P.C. Patnaik, and J.S. Tse, Elastic Properties of Multi-Component Nickel Solid Solutions, *Superalloys*, 2004, **2004**, p 753–758
24. T.D. Shen and C.C. Koch, The Influence of Dislocation Structure on Formation of Nanocrystals by Mechanical Attrition, *Mater. Sci. Forum*, 1995, **179–181**, p 17–24
25. L.E. Tyryshkina, G.A. Chiganova, and A.K. Abkaryan, Influence of Nanodiamonds on Microstructure of Nickel Coatings, *Univ. Proc. Powder Metal. Funct. Coat.*, 2014, **2**, p 54–58
26. A.K. Kuleshov, V.V. Uglov, V.M. Anishchik, and D.P. Rusalsky, Synthesis High Hardness Coatings from Nano-Sized Carbides of Niobium, Copper on Hard Alloy Wood-Cutting Tools, XIIth Int. Conference Interaction of Radiation with Solid, SEPT. 19–22 (Minsk, Belarus), *BSU Publishing Center*, 2017, **2017**, p 380–382 (**in Russian**)
27. W. Acchara, C. Zollfrank, and P. Greil, Microstructure and Mechanical Properties of WC-Co Reinforced with NbC, *Mater. Res.*, 2004, **7**(3), p 445–450
28. W. Tillmannn and S. Momeni, Tribological Development of TiCN Coatings by Adjusting the Flowing Rate of Reactive Gases, *J. Phys. Chem. Solids*, 2016, **90**, p 45–53